Journal Name

ARTICLE TYPE

Cite this: DOI: 00.0000/xxxxxxxxxx

Beyond Newton's Law of Cooling in evaluating magnetic hyperthermia performance: a device-independent procedure

Sergiu Ruta,[*a]‡ Yilian Fernández-Afonso,[b‡] Samuel E. Rannala,[c] M. Puerto Morales,[d] Sabino Veintemillas-Verdaguer,[d] Carlton Jones,[e] Lucía Gutiérrez,[*b] Roy W Chantrell,[c] David Serantes,[g,h]

Received Date
Accepted Date

DOI: 00.0000/xxxxxxxxxx

1 Magnetic nanoparticles synthesis and characterization details

Iron oxide magnetic nanoparticles were synthesized by precipitation of an iron (II) salt ($FeSO_4$) in the presence of a base (NaOH) and a mild oxidant (KNO_3) following a modified version of the synthesis described by Verges et al.[1]. The obtained particles (32.0±6.7 nm of average size, see Figure 1a) were then coated with dextran to improve their stability in water. The field-dependent magnetization of the particles showed saturation magnetization, remanent magnetization and coercive field values of ≈ 77 $Am^2/kg_{Fe_3O_4}$, ≈ 12 $Am^2/kg_{Fe_3O_4}$ and ≈ 4 kA/m, respectively (Figure 1b).

2 Fit of the initial slope with the classical methods

SLP values were calculated using the ISM, BLM and CSM for the analysis of the initial slope of the calorimetric results (Figure 1 from the manuscript and Tables 1 and 2 in this section). However, when looking in detail at the first minute of the heating curve, some differences were found among the devices. Probably associated with the lower resolution of the temperature probe of device 1, measurements performed with this device presented some "jumps" in the obtained data. A delay on the onset of the temperature increase was also observed in this case. This led to some problems associated to the calculation of the SLP value using the Initial Slope, the Box-Lucas or the Corrected Slope Methods. In particular, in the case of device 1, the Box Lucas iteration did not converge and the "L" value from the corrected slope method had a nonphysical value. These results indicated that the quality of the acquired data had a strong impact on the uncertainties associated with the SLP value calculation. Data obtained from devices 2 and 3, were smoother and did not present any problem in the fit using the three different approaches.

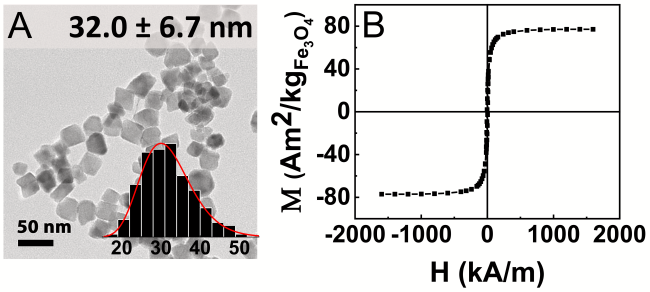

Fig. 1 Magnetic nanoparticles characterization.(A) Transmission electron microscopy image and particle size distribution histogram for nanoparticles . (B) Field dependent magnetization at room temperature (300 K) .

To fit the cooling part of figure 3 within the main text, the first approach was to impose the condition of continuity in the temperature vs. time curve (i.e. the initial T of the cooling part is the final one reached during the heating part), it is obtained $a = 0.0020$, a rather poor fit, characterised by $R^2 = 0.972$, and also directly seen by the scarce overlapping between the fitting curve (dotted blue line) and experimental data (thick solid grey line). An improvement in the fit is reached is the initial condition is not applied, so that $R^2 = 0.992$, corresponding to $a = 0.0017$. Furthermore, an even greater fit (characterised by a higher R^2 value) can be obtained if, in addition to removing the condition

[a] College of Business, Technology and Engineering, Sheffield Hallam University, United Kingdom. E-mail: sergiu.ruta@shu.ac.uk
[b] Instituto de Nanociencia y Materiales de Aragón (INMA) CSIC-Universidad de Zaragoza and CIBER-BBN, Spain. E-mail: lu@unizar.es
[c] Department of Physics, University of York, United Kingdom.
[d] Materials Science Institute of Madrid (ICMM/CSIC), Spain.
[e] nanoTherics Ltd Brookside Farm, Dig Lane, Warrington, WA2 0SH, United Kingdom.
[g] Applied Physics Department, Universidade de Santiago de Compostela, Spain
[h] Instituto de Materiais (iMATUS), Universidade de Santiago de Compostela, Spain.
‡ These authors contributed equally.

		ISM		BLM				CSM	
Devices	**Measurement**	**Slope (K/s)**	**SLP (W/g)**	**b(1/s)**	**a(K)**	**L(W/K)**	**SLP (W/g)**	**L(W/K)**	**SLP (W/g)**
Device 1	1	0.075	230	-0.01	-9.13	-0.030	201	-0.044	194
Device 1	2	0.095	287	<0.001	-192.83	-0.002	293	0.012	271
Device 2	1	0.084	254	0.01	9.68	0.042	291	0.044	295
Device 2	2	0.078	234	0.01	12.62	0.028	258	0.020	252
Device 3	1	0.081	246	<0.001	5472.70	<0.001	230	0.005	235
Device 3	2	0.078	237	0.004	18.26	0.019	246	0.024	231

Table 1 Fit parameters of the classical measurements and SLP values calculated for each measurement using the different data analysis approaches.

	ISM			BLM			CSM		
Device	**SLP Average (W/g)**	**SD (W/g)**	**RSD (%)**	**SLP Average (W/g)**	**SD (W/g)**	**RSD (%)**	**SLP Average (W/g)**	**SD (W/g)**	**RSD (%)**
Device 1	**259**	**40**	**16**	**247**	**65**	**26**	**233**	**54**	**23**
Device 2	**244**	**14**	**6**	**275**	**23**	**9**	**274**	**30**	**11**
Device 3	**242**	**6**	**3**	**238**	**11**	**5**	**233**	**3**	**1**

Table 2 SLP average, standard deviation (SD) and relative standard deviation (RSD) of the values calculated using classical measurements and classical methods.

of initial temperature, the fit is restricted to the final part of the cooling curve. In this case (green solid line in figure 3), it is obtained $a = 0.0015$, with $R^2 = 0.993$. The reason why in this range the single-exponent fitting works better is because in this range the losses do behave more in a single heat-loss channel manner, as assumed in Newton's law. This is clearly illustrated in the inset of figure 3, as the final part of the curve corresponds to a linear behaviour of the $\frac{d(\Delta T)}{dt}$ *vs.* ΔT data.)

3 Section 3. Parameters for the heat diffusion calculations

$1{\cdot}10^3$	ρ_{vess}	kg/m^3
$1{\cdot}10^3$	ρ_{wall}	kg/m^3
$4.2{\cdot}10^3$	c_{Vvess}	$J/(kgK)$
$4.2{\cdot}10^3$	c_{Vwall}	$J/(kgK)$
1000	SAR	W/g
$0.8{\cdot}10^3$	k_{vess}	$Wm^{-1}K^{-1}$
$0.8{\cdot}10^3$	k_{wall}	$Wm^{-1}K^{-1}$

Table 3 Parameters for the heat diffusion calculations.

A list detailing the parameters used in the heat diffusion calculations is provided in Table 3.

4 Standard Operating Procedure

A Standard Operating Procedure to perform the Zig-zag protocol in the case of magnetic hyperthermia experiments is described below.

1. Place the MNPs liquid suspension in the sample holder (ideally 1 mL volume at a concentration of 1 mg Fe/mL for the case of iron oxide magnetic nanoparticles).
2. Wait until the temperature is stable before turning the AC magnetic field on.
3. Turn the AC field ON and wait until the sample temperature has increased 2-3ºC.
4. Switch OFF the AC field and wait until the temperature has decreased 2ºC.
5. Turn the field ON again and repeat the cycle of heating 2-3ºC and cooling 2ºC several times times.
6. Calculate the slope of the heating and cooling curves near the peak (although this may depend on the device used for the measurements, a possible interval for this could be around 0.5 ºC).
7. Following Equation 8 from the manuscript, the SLP is calculated from the difference of the two slopes.

5 Reproducibility test

In order to check the reproducibility of repeated measurements, five different aliquots of a similar sample as described in Figure 1 but from a different batch, were characterized using Device 2 and performing a short version of the zigzag protocol in which 3 peaks were measured. The temperature variation over time of each independent sample is shown in Figure 2 together with a comparison of the SLP values calculated in the analysis of each peak using the Peak Analysis Method. Furthermore, the average SLP value calculated for each sample are compared in a bar graph. Results from these experiments indicate consistent and reproducible results when repeating the analysis of several aliquots of the same sample.

6 Control measurements using water samples

Water samples were exposed to the AC magnetic field in order to test the possible contribution of heat flux coming from the coils. A heat flux coming from the coils was detected. At very long times, this heat flux was larger for Device 2 than for Device 1. Nevertheless, for the initial time points in which the Classical Methods are generally performed (the first 60 seconds), the contribution of the heat from the coil to the water temperature was almost negligible, below 0.1 degrees.

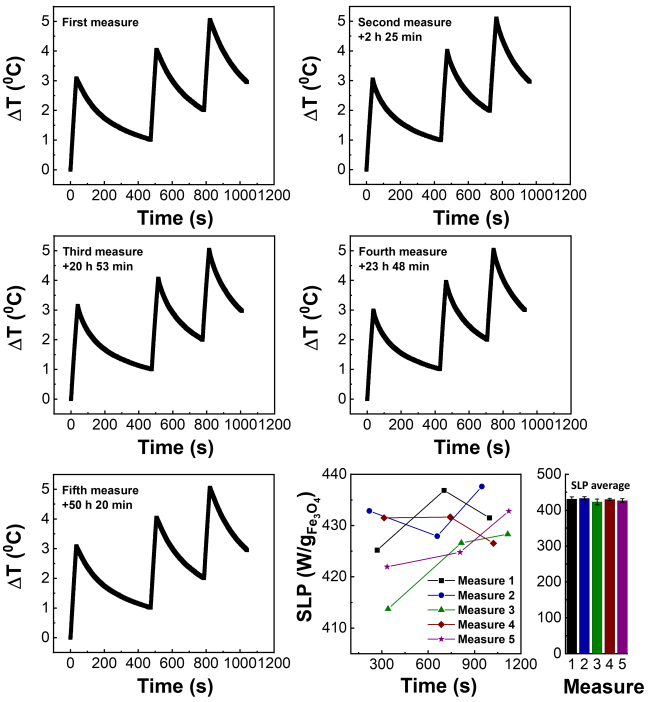

Fig. 2 Repetitions of the zig/zag measurements using Device 2. Each plot corresponds to the measurement of an independent alliquot coming from the same sample. In the last plot, SLP values calculated in the three peaks analyzed for each measurement are shown, together with the average SLP value calculated for each measurement.

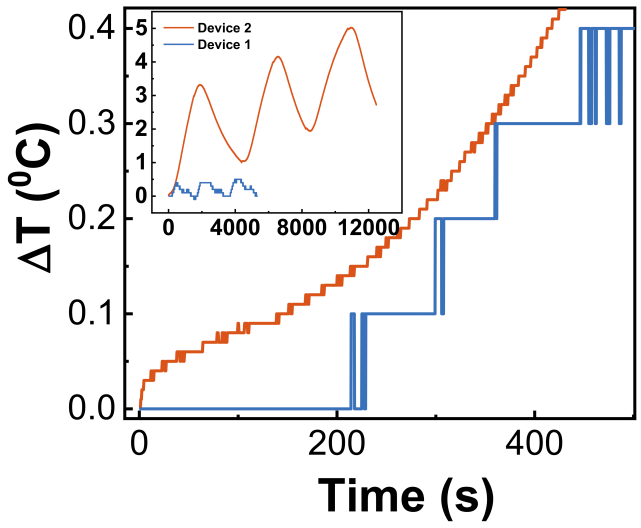

Fig. 3 Temperature variation over time of water samples tested in Devices 1 and 2 using the same AC field conditions as for the rest of the experiments. The inset shows a measurement performed during longer acquisition times.

7 SLP values calculated using the PAM

Table 4 includes the SLP values calculated for each peak analyzed using the PAM for the three Devices.

	SLP (W/g)		
Peaks	Device 1	Device 2	Device 3
Peak 1	267	251	294
Peak 2	275	249	304
Peak 3	252	254	287
Peak 4	247	251	223
Peak 5	307	260	243
Peak 6	253	261	264
Peak 7	235	272	295
Peak 8	292	260	265
Peak 9	245	264	251
Peak 10	229	273	281
Peak 11	293		266
Peak 12	246		270
Peak 13	237		251
Peak 14	301		
SLP Average	263	260	269
SD	26	8	23
RSD (%)	10	3	9

Table 4 Specific loss power (SLP) values at each peak in the ZigZag measurements and average, standard deviation (SD) and relative standard deviation (RSD of these values).

Notes and references

1 M. A. Vergés, R. Costo, A. Roca, J. Marco, G. Goya, C. Serna and M. d. P. Morales, *Journal of Physics D: Applied Physics*, 2008, **41**, 134003.